Submitted, 2014 Winter q-bio Conference (5 Nov 2013)
http://www.cds.caltech.edu/~murray/papers/guo+14-wqbio.html

Implementation And Simulation Of Phosphorylation-Based Insulator In Transcription-Translation Platform

Shaobin Guo, Enoch Yeung, Kayzad Soli Nilgiriwala, Domitilla Del Vecchio, Richard M. Murray

***Abstract*—The operational amplifier (OPAMP) is a very useful insulation module in electric circuits to avoid loading effect (retroactivity). In synthetic biological circuits, we also have the same retroactivity problem, in which the biomolecular systems are not always modular due to downstream components. The output of the upstream component will be affected as the downstream component sequesters that output, which in turn impedes the process of constructing more complex biocircuits. To address this obstacle, the retroactivity needs to be attenuated by implementing a similar OPAMP device using biocircuits. Previous theoretical papers suggested a potential function of a phosphorylation based circuit in providing the feature of attenuating retroactivity. Here we presented a successful prototyping and implementation of such a phosphorylation-based insulator (PBI) in an *in vitro* cell-free transcription-translation system (TX-TL). We demonstrated that retroactivity also exists in TX-TL system, if not stronger, by testing a simple negative regulation circuit. Besides we showed that the TX-TL system contains all the protein, DNA components and other resources required for the PBI circuit to work properly. We then demonstrated that the PBI circuit helps minimizing the loading effect to less than 10% compared to control circuit. With this preliminary PBI circuit design, attenuation of retroactivity while connecting two modules *in vitro* becomes possible. In concert with another paper from our group (E. Yeung, S. Guo, R. Murray QBIO2014) which used system identification to estimate all three essential parameters in a simplified PBI model, we showed that the simulations based on these parameters match the experimental data very well and provide an interesting insight into future designs.**

I. INTRODUCTION

The successful design and implementation of those inaugural biocircuits, such as the genetic toggle switch and the repressilator, have shown the idea of modularity in biological circuits [1], [2]. The recognition of functional modules makes building large and complicated biological circuits possible. Basic modules can be studied and tested in isolation and then could be connected with other modules to perform certain functions. However, the modularity of biological circuits could change when interconnections are made. It is called retroactivity or loading effect, which is a fundamental issue in systems engineering [3]. This means that when a downstream system is connected to another system, the downstream system will inevitably affect the behavior of upstream component. As a result, the signal generated by the upstream component cannot be effectively transferred to other components.

Retroactivity can be divided into two types based on which signal it affects, retroactivity to the input and retroactivity to the output. Based on previous theoretical studies, an operational-amplifier-like orthogonal biomolecular device could do the magic of attenuating retroactivity [3]. In an electronic operational amplifier (OPAMP), it absorbs little current from upstream; as a result, there is almost no voltage drop to upstream output. At the same time, the retroactivity to the output is attenuated because of a large amplification gain and an equally large negative feedback loop. To apply the same idea in biological circuits, we took advantage of the fast phosphorylation-dephosphorylation cycle, which previous papers suggested [3]. In this phosphorylation-based insulator design, because input signal Z is a kinase, the circuit only needs a small amount of it, which generate little retroactivity to upstream output. Concurrently, a large amplification is obtained by having abundant substrate X, which is phosphorylated by Z into X^P, only which can bind to downstream binding sites to activate transcription. An equally large negative feedback mechanism is attained by phosphatase Y which dephosphorylated X^P into X. By having this insulator, theoretically the retroactivity to both input and output can be minimized.

Here we tested an insulator design using nitrogen regulation proteins [4] in a cell-free transcription-translation (TX-TL) system [5], [6]. By using this biomolecular breadboard platform, we were able to fast assemble the circuit in linear DNAs form [ref-Zach] and fast prototype the design in a few weeks. We demonstrated that this insulator circuit helped attenuate the retroactivity to less than 10%. Besides, we also used system identification results to run some simulations, which match our experimental data well. We hope these preliminary results will contribute to future work on attenuation of retroactivity while interconnecting functional modules in vitro and in vivo.

II. RESULTS

A. Demonstration Of The Loading Effect In TX-TL

Firstly, we wanted to demonstrate loading effect in TX-TL system. The example we used is a simple negative regulation circuit, in which, constitutively expressed TetR proteins repress downstream components pTet-deGFP and pTet-RFP DNA transcription unless inducer aTc is added (Figure 1A). Here, we considered pTet-deGFP as the reporter and pTet-RFP as the load. When there is no inducer around, the reporter will be off because of repression by TetR. However, if we added a lot of load into the system, the load sequestered TetR proteins from pTet-deGFP, resulting in activation of deGFP transcription (Figure 1B). This is a consequence of retroactivity, in which downstream components affect the

behavior of the upstream system output. Then we tested this effect in the presence of different inducer concentrations (Figure 1C). At low aTc concentrations (less than $0.5\mu g/mL$), as load concentration increased, deGFP expression increased because of retroactivity. However, if too much aTc was added, deGFP expression actually decreased as load increased. This is because the resource, such as ribosomes, RNA polymerase, in TX-TL is limited.

In conclusion, the simple circuit demonstrated that there is retroactivity in biological circuits in TX-TL system. To address this problem, we would need to insert an insulator circuit between the upstream and downstream components.

B. Demonstration Of The Phosphorylation Cycle

Based on Del Vecchio group's insulator design (Figure 2A)[ref-Del Vecchio], we adapted it to a simpler form to implement in TX-TL system (Figure 2B). This is one of the most useful features of TX-TL system, which is instead of tuning promoter and ribosome bind site strength, we can simply vary the concentrations of linear DNAs added to change the behavior of the circuit. This makes circuit prototyping straightforward and fast.

The insulator design is based on a well-known two-component signal transduction system regulating the transcription of genes encoding metabolic enzymes and permeases in response to carbon and nitrogen status in *Escherichia coli* and related bacteria [7]. There are two essential proteins in the system, NRII and NRI (NtrB-NtrC). NRI can be phosphorylated into NRI^P by NRII (kinase form). Only NRI^P is able to activate the σ^{54}-dependent promoter glnA and trigger the transcription of downstream genes [8]. NRII is both a kinase and phosphatase, regulated by the PII signal transduction protein, which, on binding to NRII, inhibits the kinase activity of NRII and activates the NRII phosphatase activity [9]. NRII is known to form dimer and will autophosphorylate itself to become kinase. Previous studies suggested that when NRII has a mutation of leucine to arginine at residue 16, it loses its phosphatase activity but showed normal autophosphorylation. In contrast, NRII which has H139N mutation, is not able to transfer the phosphoryl group from its active site histidine to an aspartate side chain of NRI [7]. As a result, NRII$L16R$ only acts as a kinase and NRII$H139N$ only functions as phosphatase.

In our circuit design, proteins NRI, NRII$L16R$ and NRII$H139N$ are all constitutively expressed (although they are under lac promoter, there is not LacI to repress them in our system). Reporter deGFP is controlled by σ^{54}-dependent promoter glnA, which will be activated by phosphorylated NRI. By virtue of the fast timescale of phosphorylation and dephosphorylation loop, this circuit enjoys a large amplification gain and an equally large negative feedback mechanism as mentioned in introduction, which makes it a promising insulation device.

Before testing the insulation capability of this circuit, we need to demonstrate the phosphorylation and dephosphorylation work in TX-TL just like in vivo. As shown in Figure

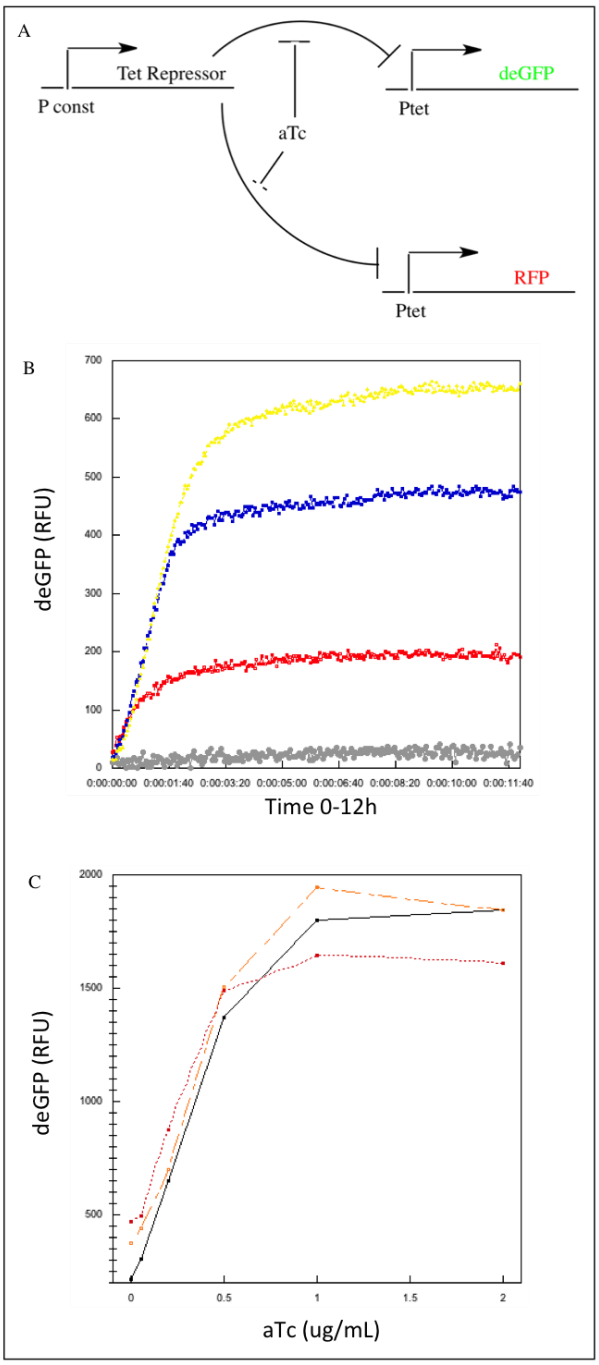

Fig. 1: **A**: The circuit used to demonstrate retroactivity (loading effect) in TX-TL system. **B**: Time course data with different concentrations of load pTet-RFP linear DNA added. All but negative control were added with $1nM$ TetR linear DNA and $8nM$ pTet-deGFP linear DNA. Gray: negative control; Red: $0nM$ load; Blue: $32nM$ load; Yellow: $64nM$ load. **C**: Inducer aTc titration with different load linear DNA added. All were added with $1nM$ TetR linear DNA and $8nM$ pTet-deGFP linear DNA. Black: $0nM$ load; Orange: $32nM$ load; Red: $64nM$ load. Data were collected using BIOTEK Synergy H1 Hybrid Multi-Mode Microplate Reader.

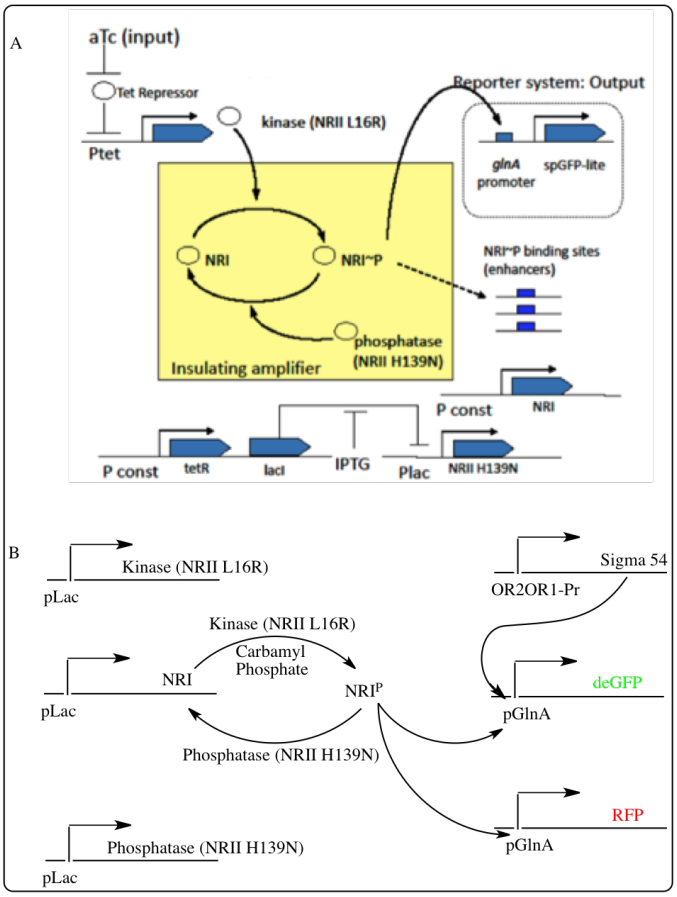

Fig. 2: **A**: Phosphorylation-based insulator circuit design by Del Vecchio group. **B**: Adapted form of the insulator for TX-TL implementation. Kinase will phosphorylate NRI into NRI^P, which together with σ^{54} will activate pGlnA. At the same time, phosphatase will dephosphorylate NRI^P into NRI.

3, as we increased the concentration of NRII$L16R$ linear DNA, we got more deGFP expression; and when we increased NRII$H139N$ linear DNA amount, less deGFP was expressed. This basically suggested that the phosphorylation cycle works in TX-TL system. We also found that σ^{54} DNA is required as there is little σ^{54} in the TX-TL cell extract and additional phosphate source is recommended but not essential (data not shown).

C. Demonstration Of The Insulation Capability Of Our Design

To test the insulation capability of our insulator, we compared the behaviors of the insulator circuit with a control circuit which doesn't have a large amplification gain, neither a negative feedback loop. As mentioned in previous theoretical studies [3], the insulator circuit requires abundant substrate NRI to achieve high gain. So we added $47.5nM$ NRI linear DNA in insulator circuit and only $5nM$ in control circuit. But to take resource limitation into account, we balanced the insulator and control by adding $42.5nM$ of junk DNA

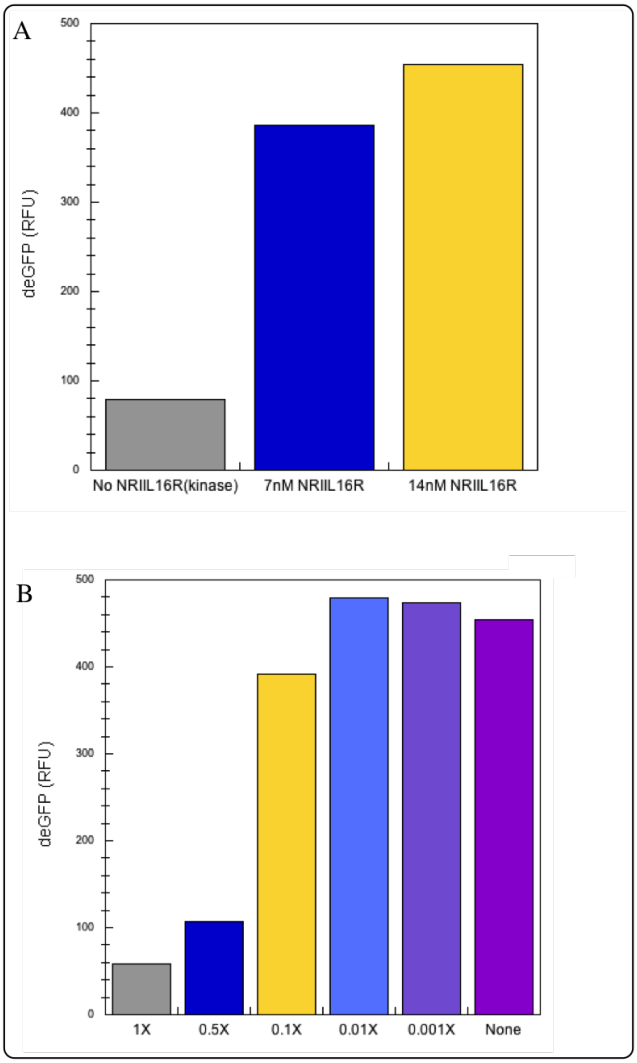

Fig. 3: **A**: Effect of varied concentrations of NRII$L16R$(kinase) DNA on deGFP expression. All the reactions contained $10nM$ pGlnA-deGFP, $3.25nM$ σ^{54} and $10nM$ NRI linear DNAs in addition of $10mM$ carbamyl phosphate. Gray: negative control; Blue: $7nM$ NRII$L16R$ DNA; Yellow: $14nM$ NRII$L16R$ DNA. **B**: Effect of different concentrations of NRII$H139N$ DNA on deGFP expression. All the reactions contained $10nM$ pGlnA-deGFP, $3.25nM$ σ^{54}, $10nM$ NRI and $14nM$ NRII$L16R$ linear DNAs in addition of $10mM$ carbamyl phosphate. X-axis is the ratio of NRII$H139N$:NRII$L16R$.

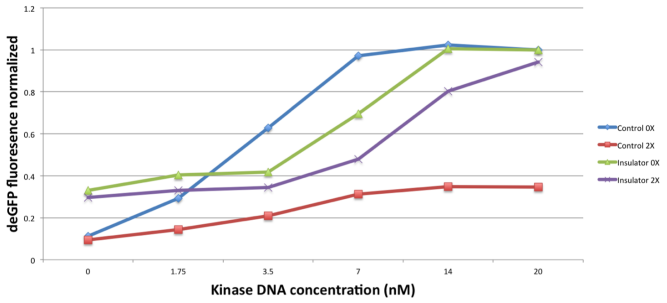

Fig. 4: **A**: Transfer curve of the control and insulator circuits with and without downstream load. Control: $10nM$ pGlnA-deGFP, $5nM$ sigma54, $10mM$ CP, $5nM$ NRI, 0 or $20nM$ pGlnA-RFP and $42.5nM$ junk DNA to balance the resource limitation as in insulator circuit. Insulator: $10nM$ pGlnA-deGFP, $5nM$ sigma54, $10mM$ CP, $47.5nM$ NRI, 0 or $20nM$ pGlnA-RFP and 1nM NRII$H139N$.

(pTet-RFP) in the control circuit. Then we varied the amount of downstream glnA promoters by adding $0nM$ (0X) or $20nM$ (2X) pGlnA-RFP linear DNA, which would introduce retroactivity. We then titrated with different concentrations of NRII$L16R$ (kinase) linear DNAs. Data were collected using BIOTEK Synergy H1 Hybrid Multi-Mode Microplate Reader. Then the deGFP relative fluorescence unit of the control and insulator circuits were normalized using their 0X RFU readings, respectively. As shown in Figure 4, when control circuit was added 2X load, the deGFP expression dropped significantly (more than 60%). In contrast, the insulator circuit only showed 10% 20% decrease in the deGFP expression when 2X load was added. These results suggested that the insulator does help attenuate the retroactivity in biological circuits in TX-TL platform.

D. Simulation

In collaboration with Enoch Yeung of our group, we performed a comprehensive system identification of the PBI circuit in another report (E. Yeung, S. Guo, R. Murray QBIO2014). We came up with a simplified PBI model, which consists of all the essential chemical reactions involving in the process:

$$\mathrm{NRI} + \mathrm{K} \xrightarrow{k_{\mathrm{ph}}} \mathrm{NRI^P} + \mathrm{K}$$
$$\mathrm{NRI^P} + \mathrm{Ph} \xrightarrow{k_{\mathrm{deph}}} \mathrm{NRI} + \mathrm{Ph}$$
$$\mathrm{NRI^P} + \mathrm{pGlnA} \xrightarrow{k_{\mathrm{cat}}} \mathrm{NRI^P} + \mathrm{pGlnA} + \mathrm{deGFP}$$
$$\mathrm{NRI^P} + \mathrm{pGlnA_{Load}} \xrightarrow{k_{\mathrm{cat}}} \mathrm{NRI^P} + \mathrm{pGlnA_{Load}} + \mathrm{RFP}$$
$$\mathrm{NRI^P} \xrightarrow{k_{\mathrm{auto}}} \mathrm{NRI}$$

where we made the following assumption that protein concentrations of kinase, phosphatase and substrate remain almost unchanged:

In a set (t - ε, t+ ε)

$$K^{tot} = K, Ph^{tot} = Ph, NRI^{tot} = NRI^P + NRI$$

where,

$$||K^{tot}(t+\varepsilon) - K^{tot}(t-\varepsilon)|| < 0(\varepsilon)$$
$$||Ph^{tot}(t+\varepsilon) - Ph^{tot}(t-\varepsilon)|| < 0(\varepsilon)$$
$$||NRI^{tot}(t+\varepsilon) - NRI^{tot}(t-\varepsilon)|| < 0(\varepsilon)$$

Based on the reactions and assumptions above, we derived the following differential equations indicating the rates of change for proteins NRI and deGFP:

$$\dot{NRI^P} = -k_{auto}NRI^P + k_{ph}(NRI^{tot} - NRI^P)K^{tot} - k_{deph}Ph^{tot}NRI^P$$

$$\dot{deGFP} = k_{cat}\frac{NRI^P p^{tot}_{\mathrm{GlnA}}/k_M}{1 + (p^{tot}_{\mathrm{GlnA}} + p^{tot}_{\mathrm{GlnALoad}})/k_M}$$

When the reactions are at steady state, the concentration of protein NRI should remain steady, so we have:

$$0 = \dot{NRI^P} = -k_{auto}NRI^P + k_{ph}(NRI^{tot} - NRI^P)K^{tot} - k_{deph}Ph^{tot}NRI^P$$

which gives us:

$$NRI^P = \frac{k_{ph}NRI^{tot}K^{tot}}{k_{ph}K^{tot} + k_{auto} + k_{deph}Ph^{tot}}$$

then we have:

$$\dot{deGFP} = k_{cat}\frac{\theta p^{tot}_{\mathrm{GlnA}}/k_M}{1 + (p^{tot}_{\mathrm{GlnA}} + p^{tot}_{\mathrm{GlnALoad}})/k_M}$$

where θ is given as

$$\theta(NRI^{tot}, K^{tot}, Ph^{tot}) = \frac{k_{ph}NRI^{tot}K^{tot}}{k_{ph}K^{tot} + k_{auto} + k_{deph}Ph^{tot}}$$

As the autophosphatase activity of NRI$^{\mathrm{P}}$ is fairly slow compared to the dephosphorylation by phosphatase NRII$H139N$ [10], we can simplify θ by approximating k_{auto} = 0:

$$\theta = \frac{(k_{ph}/k_{deph})NRI^{tot}}{k_{ph}/k_{deph} + Ph^{tot}/K^{tot}}$$

Then we determined the three parameters – k_{cat}, k_M and k_{ph}/k_{deph} (Table 1) – using system identification (details shown in previously mentioned report). We also estimated the protein concentration of NRI^{tot} at $t = 120min$ by measuring the protein concentration of deGFP using the exact same promoter at $t = 120min$ and taking into account the differences between these two proteins in terms of transcription, translation and maturation rates. The reason to choose $t = 120min$ was that after this time point, mRNA concentration would start decreasing gradually as the transcription-translation machinery began to lose functionality (data shown in previous mentioned report). Besides, data used to do system identification showed certain extent of linearity between the start of the reactions and $t = 120min$, which we used to estimate the rate of reporter (deGFP) production. Because of

TABLE I: Estimation for k_{cat}, k_M, k_{ph}/k_{deph} and $NRI^{tot}(t = 120min)$

	Value	Unit
k_{cat}	0.0974	s^{-1}
k_M	1.5762	nM
k_{ph}/k_{deph}	0.0981	$dimentionless$
NRI^{tot}	68	nM

these, all the following simulations were limited to 2 hours of duration.

To start, we performed some simulations to verify the parameters by comparing them to the experimental data. The first simulation was testing how the ratio of phosphatase over kinase would affect the output of the PBI circuit. As shown in Figure 5A, when Ph^{tot}/K^{tot} increased, deGFP level decreased. Comparing Figure 5B with Figure 3B, we can see that they showed the exact same trend when changing Ph^{tot}/K^{tot}. This shows that the simulation results are consistent with experimental data on the role of Ph^{tot}/K^{tot} playing in the PBI circuit.

Then we wanted to know how would different initial conditions affect the output. We swept different initial conditions for the reporter pGlnA-deGFP, the load pGlnA-RFP and phosphatase over kinase ratio (Ph^{tot}/K^{tot}) and results were shown in Figure 6. In Figure 6A, we swept [pGlnA-deGFP] and [pGlnA-RFPload]. As we can see in the surface plot, more reporter DNA results in more deGFP level, which is obvious. And more load DNA brings down the deGFP level, which is a result of retroactivity as load DNA competes with reporter DNA for transcription and translation resources, such as RNA polymerases and ribosomes. Load DNA or mRNA sequesters those resources away from reporter DNA or mRNA, ending up with less reporter protein made. In Figure 6B, we changed the concentration of the load pGlnA-RFP and the ratio of Ph^{tot}/K^{tot}. As we mentioned above, when certain amounts of phosphatase and kinase are added, the PBI circuit will have a high gain because of phosphorylation and an equally large negative feedback by dephosphorylation. As a result, retroactivity from downstream load will be attenuated. The simulation results in Figure 6B just showed the exact same idea. When Ph^{tot}/K^{tot} is very small, there isn't a strong negative feedback to complement the high gain. Then when there is too much load, the output will decrease significantly. However, when Ph^{tot}/K^{tot} is high, the loading effect will be much less significant as the negative feedback converts the excessive activator NRI^P back to inactive form. Through this mechanism, retroactivity is largely attenuated.

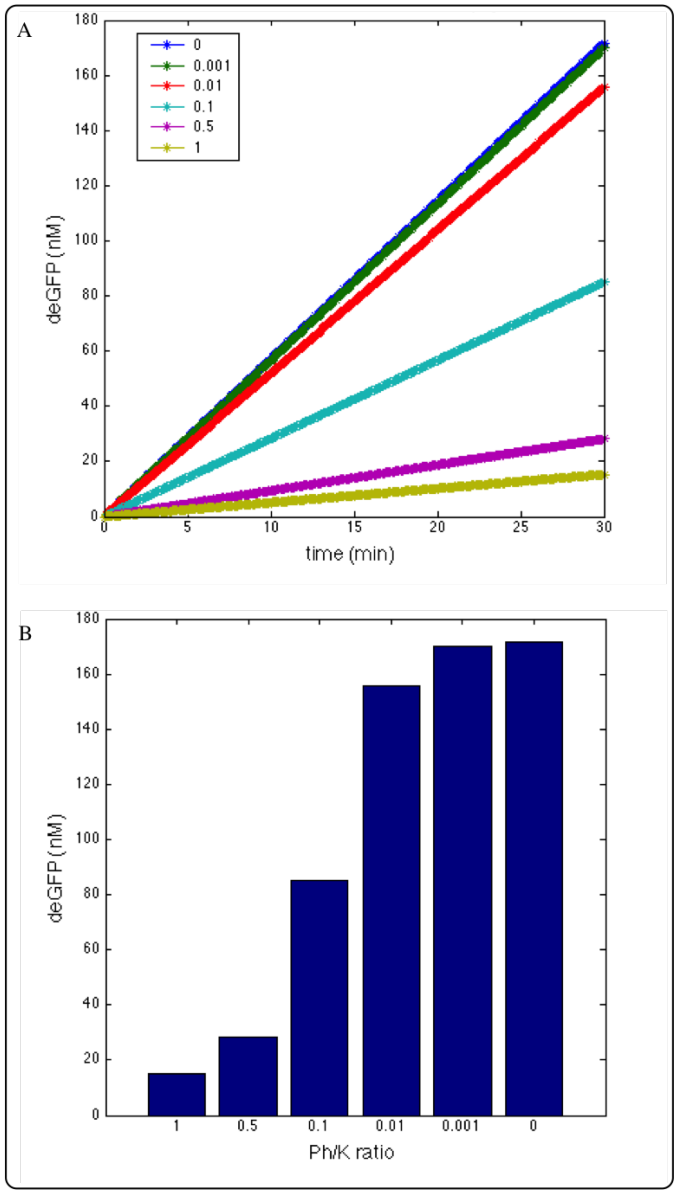

Fig. 5: **A**: PBI model simulation using estimated parameters. Initial condition: $10nM$ DNA pGlnA-deGFP and $68nM$ protein NRI^{tot} with Ph^{tot}/K^{tot} varying between 0 and 1. No load added. Simulation time is $30min$. **B**: The expression levels of deGFP when different Ph^{tot}/K^{tot} ratios were used. $t = 30min$ data points shown.

III. Conclusions And Future Work

Previously when researchers tried to build a complex circuit, some time-consuming tuning work was required as interconnecting different modules would result in changes of outputs or inputs. To streamline this process, we looked into circuits which might provide some insulation features. We would like to put this kind of device between upstream and downstream modules to accommodate the changes in outputs or inputs. Inspired by Del Vecchio group, we assembled a simplified PBI circuit *in vitro* and fast prototyped in our TX-TL biomolecular breadboard. The results were very exciting as we could attenuate the retroactivity caused by downstream components to a satisfying level (less than 10%). Our work on the *in vitro* implementation of the PBI circuit showed a very promising future for constructing more complicated biocircuits which might consist of several individual functional modules.

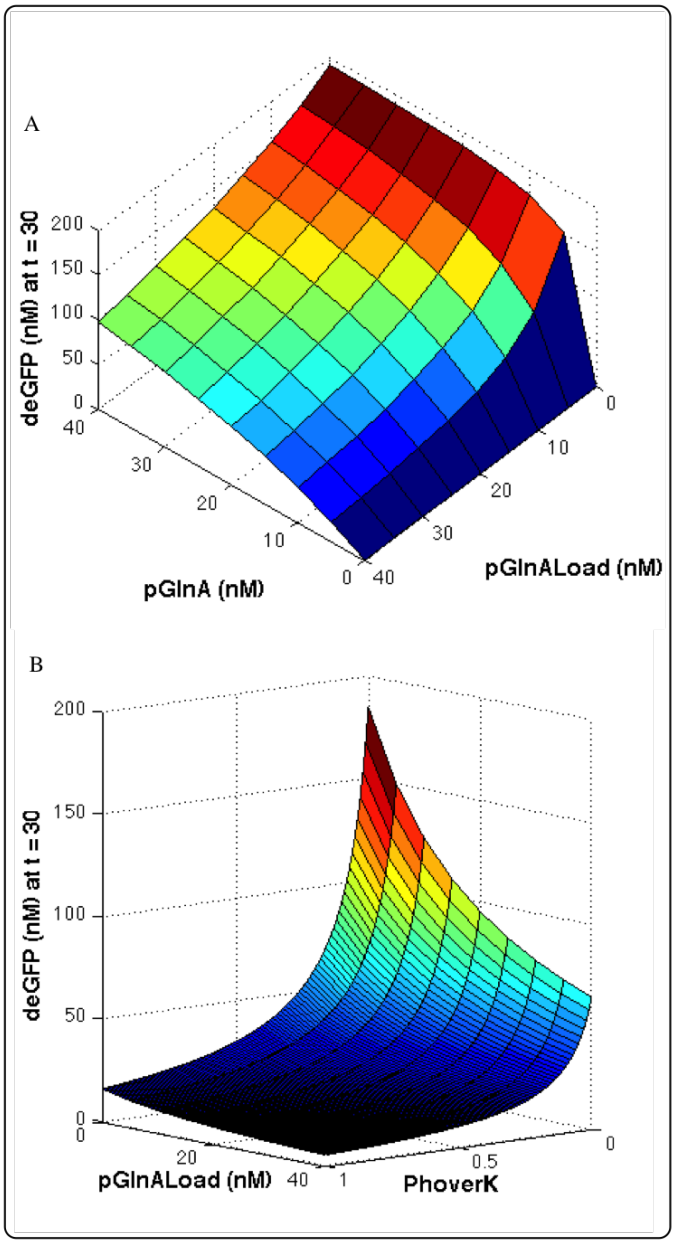

Fig. 6: **A**: PBI model simulation using estimated parameters. Initial condition: DNA pGlnA-deGFP ranging from 0 to 40 nM and DNA pGlnA-RFP (load) ranging from 0 to 40 nM, with $68nM$ protein NRI^{tot} and Ph^{tot}/K^{tot}=0. Simulation time is $30min$. **B**: Initial condition: DNA pGlnA-RFP (load) ranging from 0 to 40 nM and Ph^{tot}/K^{tot} varying between 0 and 1, with 20 nM DNA pGlnA-deGFP and $68nM$ protein NRI^{tot}. Simulation time is $30min$.

Besides, our simulations results based on parameters estimated by system identification confirmed our conclusions from experimental data and previous theoretical predictions. These *in silico* results also showed the power of computational biology and its future applications in guiding biological experiments and synthetic biocircuits design.

In terms of implementing the PBI circuit in cells, our collaborator Del Vecchio group is working on the in vivo implementation of the PBI circuit and have gotten some very promising data.

Next step for us would be implementing the circuit between two functional modules in TX-TL. But TX-TL breadboard has its limitations when doing the assays by hands as human beings cannot pipette more than 40 reactions without evaporating 1-2μL of the whole $10\mu L$ reactions, and transcription and translation can only go on for 2 hours before resource limitation kicks in. So we will utilize other advanced equipments such as the liquid handling robot and ALL (Advanced Liquid Logic) to help refine the prototyping and implementation of the PBI circuit in TX-TL platform.

REFERENCES

REFERENCES

[1] Timothy S Gardner, Charles R Cantor, and James J Collins, "Construction of a genetic toggle switch in escherichia coli", *Nature*, vol. 403, no. 6767, pp. 339–342, 2000.

[2] Michael B Elowitz and Stanislas Leibler, "A synthetic oscillatory network of transcriptional regulators", *Nature*, vol. 403, no. 6767, pp. 335–338, 2000.

[3] Domitilla Del Vecchio, Alexander J Ninfa, and Eduardo D Sontag, "Modular cell biology: retroactivity and insulation", *Molecular systems biology*, vol. 4, no. 1, 2008.

[4] Alexander J Ninfa and Mariette R Atkinson, "Pii signal transduction proteins", *Trends in microbiology*, vol. 8, no. 4, pp. 172–179, 2000.

[5] Jonghyeon Shin and Vincent Noireaux, "An e. coli cell-free expression toolbox: application to synthetic gene circuits and artificial cells", *ACS synthetic biology*, vol. 1, no. 1, pp. 29–41, 2012.

[6] ZZ Sun, CA Hayes, J Shin, F Caschera, RM Murray, and V Noireaux, "Protocols for implementing an escherichia coli based tx-tl cell-free expression system for synthetic biology.", *Journal of visualized experiments: JoVE*, , no. 79, 2012.

[7] Augen A Pioszak and Alexander J Ninfa, "Genetic and biochemical analysis of phosphatase activity of escherichia coli nrii (ntrb) and its regulation by the pii signal transduction protein", *Journal of bacteriology*, vol. 185, no. 4, pp. 1299–1315, 2003.

[8] Alexander J Ninfa, Lawrence J Reitzer, and Boris Magasanik, "Initiation of transcription at the bacterial glnap2 promoter by purified e. coli components is facilitated by enhancers", *Cell*, vol. 50, no. 7, pp. 1039–1046, 1987.

[9] Alexander J Ninfa and Boris Magasanik, "Covalent modification of the glng product, nri, by the glnl product, nrii, regulates the transcription of the glnalg operon in escherichia coli", *Proceedings of the National Academy of Sciences*, vol. 83, no. 16, pp. 5909–5913, 1986.

[10] Augen A Pioszak and Alexander J Ninfa, "Mutations altering the n-terminal receiver domain of nri (ntrc) that prevent dephosphorylation by the nrii-pii complex in escherichia coli", *Journal of bacteriology*, vol. 186, no. 17, pp. 5730–5740, 2004.